



# Photocatalytic reduction of CO<sub>2</sub> on Cu<sub>2</sub>O-loaded Zn-Cr layered double hydroxides



Haoyang Jiang<sup>a</sup>, Ken-ichi Katsumata<sup>b,\*</sup>, Jeongsoo Hong<sup>c</sup>, Akira Yamaguchi<sup>a</sup>, Kazuya Nakata<sup>b</sup>, Chiaki Terashima<sup>b</sup>, Nobuhiro Matsushita<sup>a</sup>, Masahiro Miyauchi<sup>a</sup>, Akira Fujishima<sup>b</sup>

<sup>a</sup> Department of Materials Science and Engineering, Tokyo Institute of Technology, 2-12-1 Ookayama, Meguro-ku, Tokyo 152-8552, Japan

<sup>b</sup> Photocatalysis International Research Center, Tokyo University of Science, 2641 Yamazaki, Noda-shi, Chiba 278-8510, Japan

<sup>c</sup> Advanced Ceramics Research Center, Nagoya Institute of Technology, Gokiso, Showa-ku, Nagoya-shi, Aichi 466-8555, Japan

## ARTICLE INFO

### Keywords:

Photocatalytic reduction of CO<sub>2</sub>  
Layered double hydroxides  
Cu<sub>2</sub>O  
Electron trap

## ABSTRACT

A series of Cu<sub>2</sub>O-loaded Zn-Cr layered double hydroxides (LDHs) was prepared via an *in situ* reduction process from Cu-Zn-Cr ternary LDHs and applied to the photoreduction of CO<sub>2</sub>. The formation of Cu<sub>2</sub>O nanoparticles and the preservation of the LDH structure was confirmed by X-ray diffraction and transmission electron microscopy. Among the loaded LDHs, the 0.1Cu<sub>2</sub>O@Zn<sub>1.8</sub>Cr LDH exhibited optimal activity for the conversion of CO<sub>2</sub> into CO in pure water and was superior to both the corresponding Cu-Zn-Cr ternary LDH and pristine Zn<sub>2</sub>Cr LDHs. In addition, the production of CO was further promoted by increasing the solubility of CO<sub>2</sub> using a nano-bubble solution instead of pure water. The loaded Cu<sub>2</sub>O nanoparticles probably function as effective electron traps, promoting charge separation and providing active sites for CO<sub>2</sub> reduction.

## 1. Introduction

Layered double hydroxides (LDHs, [M<sub>1-x</sub><sup>2+</sup>M<sub>x</sub><sup>3+</sup>(OH)<sub>2</sub>]<sup>z+</sup>(A<sup>n-</sup>)<sub>z/n·mH<sub>2</sub>O), a series of stacked layered clay materials, have aroused widespread attention for their unique and selective photoreduction properties, converting CO<sub>2</sub> into CO via a two-electron process under ultraviolet irradiation. The basic structure of LDHs includes cationic brucite-like host layers consisting of coordinated MO<sub>6</sub> octahedrons with shared edges, and anionic guest species, commonly CO<sub>3</sub><sup>2-</sup>, in the interlayer regions to compensate for the insufficient charge and yield electric neutrality [1–3]. Izumi et al. [4] reported that CO<sub>2</sub> was photocatalytically reduced to methanol and CO by using H<sub>2</sub> as a reductant on Zn-Cu-Al and Zn-Cu-Ga LDHs. Teramura et al. [5] achieved the photocatalytic conversion of CO<sub>2</sub> into CO and O<sub>2</sub> in pure water using a series of LDHs and found that Cl<sup>-</sup> can improve the activity and selectivity of the LDH by acting as an effective hole scavenger in Ni-based LDHs [6–8].</sub>

Although many kinds of LDH photocatalysts have been developed, there is still a chasm between expectation and actual performance. Surface decoration on the photocatalyst with a cocatalyst is believed to be important to achieve enhanced photocatalytic activity because the cocatalyst not only extracts the photogenerated charge carriers but also provides reaction sites for gas evolution [9,10]. Previously, we have developed noble metal (Pt, Pd, and Au)-loaded LDHs that show improved CO<sub>2</sub> photoreduction performance, but their CO formation rates

are limited [11]. Besides, LDHs belong to amphoteric hydroxides are chemically unstable under the strongly acidic and basic conditions used during noble metal cocatalyst loading. Therefore, the development of a cost effective and easily synthesized cocatalyst is a significant but challenging task for the theoretical study and practical use of LDH-derived photocatalysts.

For CO<sub>2</sub> photoreduction, compared to noble metals, which are extensively used in water splitting reactions, copper is a cheap and abundant element and an excellent candidate for highly efficient cocatalysts. Tseng et al. [12] prepared a copper-loaded TiO<sub>2</sub>, and methanol was favorably produced on the catalysts in an aqueous CO<sub>2</sub> solution under UV irradiation. In this system, Cu<sup>I</sup> was suggested to be the active site. Zhai et al. [13] developed a Pt@Cu<sub>2</sub>O binary cocatalyst with a core-shell structure and proposed that the Cu<sub>2</sub>O shell provided sites for the preferential conversion of CO<sub>2</sub> to CH<sub>4</sub> and CO. Miyauchi et al. [14,15] discovered amorphous Cu<sup>II</sup> nanoclusters that function as efficient cocatalysts for both the electrocatalytic and photocatalytic reduction of CO<sub>2</sub> to CO. The grafting of Cu<sup>II</sup> nanoclusters onto exfoliated layered niobate and SrTiO<sub>3</sub> nanorods promoted CO generation. The formation of a Cu<sup>II</sup>-Cu<sup>I</sup> intermediate was detected and considered to be the reason for the improved photocatalytic activity. In addition, Hsu et al. [16] confirmed Cu<sub>2</sub>O can accept and accumulate electrons from the semiconductor in a heterostructure system, revealing Cu<sub>2</sub>O is qualified for the multi-electron process in CO<sub>2</sub> reduction.

\* Corresponding author.

E-mail address: [k.katsumata@rs.tus.ac.jp](mailto:k.katsumata@rs.tus.ac.jp) (K.-i. Katsumata).

Copper oxides can be synthesized by soft chemical methods; for example, Cu<sub>2</sub>O particles can be easily obtained by the chemical reduction of Cu<sup>II</sup> species using reducing agents such as reducing sugars, ascorbic acid, hydroxylamine hydrochloride, and hydrazine hydrate [17–20]. Cu-containing ternary LDHs, with Cu(OH)<sub>6</sub> units incorporated in the layered structure, are reasonable precursors to prepare Cu<sub>2</sub>O. Interestingly, only the highly dispersed Cu<sup>2+</sup> ions are separated out from the host layers via the *in situ* reduction process, and the remainder of the bimetallic ions maintain the basic structure of the LDH. Komarneni et al. [21] reported the synthesis of Cu<sub>2</sub>O-MgAl LDH composites from Mg-Cu-Al LDHs by such a method. The nano-sized Cu<sub>2</sub>O particles acted as photocatalysts for the degradation of orange II under visible light, but the function of the Mg-Al LDHs is that of a supporter and dispersant. The synergistic effect of Cu<sub>2</sub>O and photocatalytically active LDH species containing transition metals has not been confirmed. It is expected that dispersed Cu<sub>2</sub>O nanoparticles synthesized by an *in situ* reduction method can serve as cocatalysts to enhance the CO<sub>2</sub> reduction ability of LDH photocatalysts effectively. Zn-Cr LDHs are rising stars among these materials because of their excellent light harvesting properties and multi-functionality for various kinds of photocatalytic reaction [11,22–26]. Furthermore, the similar ionic radii of Cu<sup>2+</sup> (73 pm) and Zn<sup>2+</sup> (74 pm) allowed Cu(OH)<sub>6</sub> units to be easily embedded into the Zn-Cr LDH lattice [27,28].

In the present work, an *in situ* reduction approach was applied in the preparation of Cu<sub>2</sub>O-decorated Zn-Cr LDHs from Cu-Zn-Cr ternary LDHs, and the Cu<sub>2</sub>O loading enhanced the photocatalytic performance for the reduction of CO<sub>2</sub> based on comparative studies with a closed aqueous system under UV-light irradiation. A possible electron pathway during the photocatalytic reaction is also discussed in this paper.

## 2. Experimental

### 2.1. Catalyst preparation

ZnCl<sub>2</sub> was purchased from Kanto Chemical Co., Inc., and the other chemicals were commercially available reagents from Wako Pure Chemical Industries, Ltd. Ultrapure water was produced by Milli-Q® Advantage A10 water purification system. The bare Zn<sub>2</sub>Cr binary and Cu<sub>2</sub>·Zn<sub>2-2x</sub>Cr ternary LDH ( $x = 0.05, 0.10, 0.20$ , and  $0.40$ ) were synthesized by the co-precipitation method [29]. In detail,  $20 \times \text{mmol}$  ( $x = 0, 0.05, 0.10, 0.20$ , and  $0.40$ ) of CuCl<sub>2</sub>·2H<sub>2</sub>O,  $20 - 20 \times \text{mmol}$  of ZnCl<sub>2</sub>, and  $10 \text{ mmol}$  of CrCl<sub>3</sub>·6H<sub>2</sub>O were dissolved in  $15 \text{ mL}$  water to form a solution (Solution A). A mixed aqueous solution (Solution B) of NaOH-Na<sub>2</sub>CO<sub>3</sub> (2:1 molar ratio,  $[\text{Na}^+] = 4 \text{ mol/L}$ ) was prepared. Solution A and Solution B were added dropwise into  $20 \text{ mL}$  of ultrapure water via variable-flow peristaltic pumps (Fisher Scientific) with rapid stirring to form purple or blue slurries. The pH was maintained at 8.9–9.1 by controlling the speed of addition. After co-precipitation, the slurry was aged in a water bath at 333 K for 24 h. Then the precipitate was centrifuged and washed with water repeatedly (at least three times). The LDH powder was obtained by grinding the precipitate after drying at 353 K in an oven overnight.

Cu<sub>2</sub>O-loaded Zn-Cr LDHs were synthesized by performing the *in situ* reduction of the Cu<sub>2</sub>·Zn<sub>2-2x</sub>Cr LDH ( $x = 0.05, 0.10, 0.20$ , and  $0.40$ ) precursor, which was prepared as described previously. Note that the precursor should be washed but not dried. The wet precipitate was dispersed in  $50 \text{ mL}$  water, and added dropwise to  $50 \text{ mL}$  of a  $0.1 \text{ mol/L}$  ascorbic acid aqueous solution of which the pH had been adjusted to 8.9–9.1 with a NaOH-Na<sub>2</sub>CO<sub>3</sub> mixed solution (2:1 molar ratio,  $[\text{Na}^+] = 4 \text{ mol/L}$ ). The suspension was continuously stirred for 2 h at room temperature. Then the product was centrifuged and washed with water repeatedly (at least three times). The powder sample was obtained by grinding the precipitate after drying at 353 K in an oven overnight. The as-prepared Cu<sub>2</sub>O loaded LDHs are denoted ‘ $x\text{Cu}_2\text{O}@Zn_{2-2x}\text{Cr LDH}$ ’, where  $x = 0.05, 0.10, 0.20$ , or  $0.40$ .

### 2.2. Characterization

The crystallographic phases of the as-prepared samples were investigated by X-ray diffraction analysis (XRD) using a Rigaku Ultima IV diffractometer with Cu K $\alpha$  radiation ( $\lambda_{\text{K}\alpha 1} = 1.540598 \text{ \AA}$ ,  $\lambda_{\text{K}\alpha 2} = 1.544426 \text{ \AA}$ ,  $\text{K}\alpha 2/\text{K}\alpha 1 = 0.4970$ ) and a D/teX Ultra detector. Fourier transform infrared (FT-IR) spectra of the samples were measured using a JEOL JIR-7000 at room temperature in the range of 400–4000 cm<sup>-1</sup>. Samples were prepared in KBr pellets, and the spectrum of an empty KBr pellet was used as a reference. The morphology of the catalysts was observed using a Hitachi H8100 transmission electron microscope (TEM). The N<sub>2</sub> adsorption–desorption isotherms at 77 K were determined using a BELSORP 18 gas sorption analyzer. The optical absorption properties of powders in the wavelength range of 200–800 nm were recorded using the diffuse reflectance (DRS) method and a Hitachi U-3310 UV-vis spectrophotometer.

### 2.3. Photocatalytic reaction

The photocatalytic properties for CO<sub>2</sub> reduction were evaluated by liquid-phase reaction under UV irradiation if not stated otherwise. In detail, 200 mg of catalyst was dispersed in 50 mL pure water in a glass reactor with 290 mL dead volume covered by a quartz plate. After being degassed by a vacuum pump for 10 min, CO<sub>2</sub> gas was bubbled through the water and purged into the reactor for 15 min. Then, the sealed reactor was placed beneath one of the two branched guidance fibers connected to a 200-W Hg-Xe lamp (LA-310UV, Hayashi Watch-works) and irradiated for 24 h. The yields of carbon-containing compounds were detected by a gas chromatograph with a flame ionization detector (GC-FID; Shimadzu GC-2014AF equipped with 1-m ShinCarbon ST 50/80 column and a methanizer unit). The yield of H<sub>2</sub> was detected by a chromatograph with thermal conductivity detector (GC-TCD; Shimadzu GC-2014AE equipped with a 6-m ShinCarbon ST 50/80 column). The control experiments were performed by using Ar gas instead of CO<sub>2</sub> gas under the same reaction conditions. The effect of additives on the photocatalytic properties was investigated by using 0.1 mol/L aqueous Na<sub>2</sub>SO<sub>4</sub>, Na<sub>2</sub>CO<sub>3</sub>, and NaCl solutions and a commercial CO<sub>2</sub> ultra-fine bubble (UFB) solution instead of pure water. To verify the oxygen production and distinguish it from the carbon source, isotope tests were performed in a 1-cm quartz cuvette with a threaded cap. The isotope reagents were purchased from Sigma-Aldrich Co., LLC. Briefly, 50 mg 0.1Cu<sub>2</sub>O@Zn<sub>1.8</sub>Cr LDH was impregnated with 1 mL H<sub>2</sub><sup>18</sup>O, and <sup>13</sup>CO<sub>2</sub> gas was bubbled through the suspension for 20 min. Then the cuvette was sealed and irradiated with UV light for 24 h. The gas in the headspace before, during, and after irradiation was analyzed by a gas chromatography–mass spectrometry system (GC-MS; Shimadzu GCMS-QP2010).

## 3. Results and discussion

### 3.1. Catalyst characterization

Fig. 1(a) shows the XRD patterns of all the as-prepared samples including bare Zn<sub>2</sub>Cr LDH, bare Cu<sub>2</sub>O, Cu-Zn-Cr ternary LDHs, and Cu<sub>2</sub>O-loaded Zn-Cr LDHs. Characteristic of stacked layered structures, intense diffraction peaks around  $2\theta = 11.6^\circ$  and  $23.3^\circ$  were present in all the LDH samples and were assigned to the (003) and (006) lattice planes, respectively. The  $d_{003}$  value represents the interlayer spacing, and parameter  $c$  can be calculated using the equation  $c = 3d_{003}$  because typical Zn-based LDHs belong to the 3R polytype [30]. The calculated results for parameter  $c$  are in agreement with those of CO<sub>3</sub><sup>2-</sup>-type LDHs reported previously [31].

Fig. 1(b) shows the detailed scan from 58 to 62°, containing the diffraction peaks corresponding to the (110) and (113) planes, of which the position depends on the radius of metal ions within the host layers. The parameter  $a$ , which is also the cation–cation distance, can be

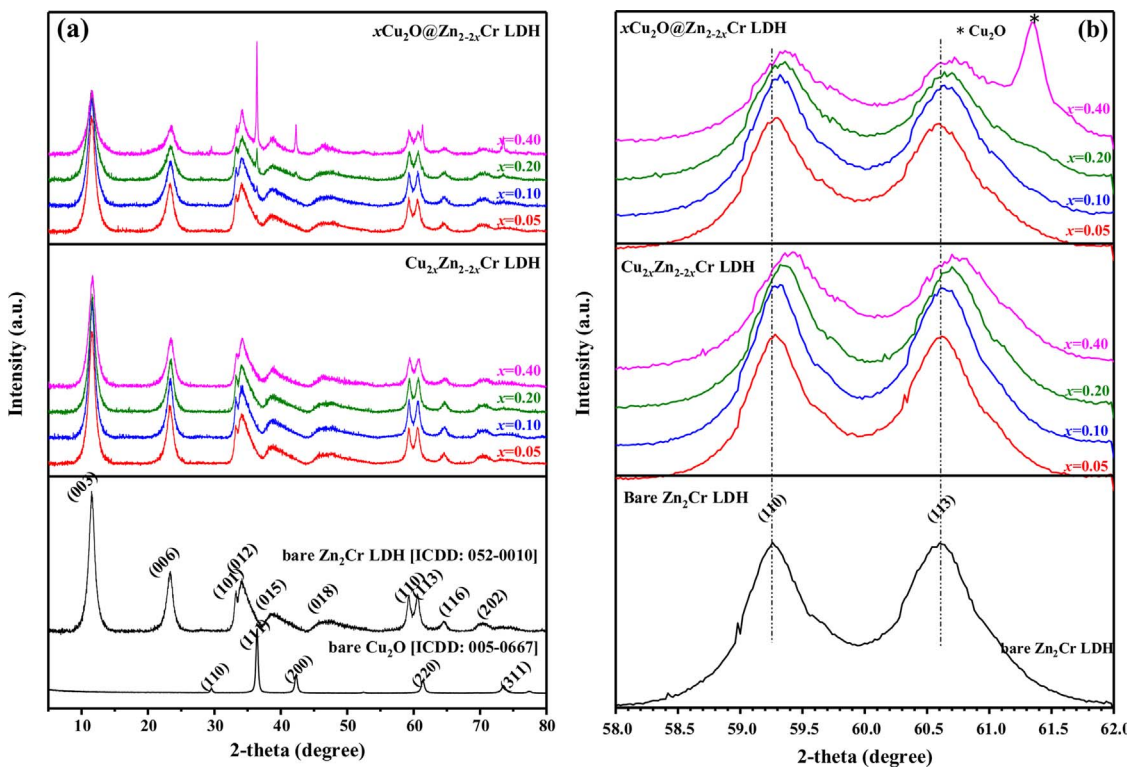


Fig. 1. XRD patterns of the as-prepared  $\text{Cu}_2\text{O}$ -loaded Zn-Cr LDHs, Cu-Zn-Cr LDHs, bare  $\text{Zn}_2\text{Cr}$  LDH, and bare  $\text{Cu}_2\text{O}$ : (a) wide scan:  $2\theta = 2\text{--}80^\circ$  and (b) detailed scan:  $2\theta = 58\text{--}62^\circ$ .

calculated from the equation  $a = 2d_{110}$ . In Cu-Zn-Cr ternary LDHs, with increasing  $\text{Cu}^{2+}/\text{M}^{2+}$  substitution ( $x$ ), the positions of the (110) and (113) peaks shifted to wider angles gradually, indicating the shrinkage of  $a$ . This result demonstrates the smooth incorporation of  $\text{Cu}^{2+}$  into the LDH host layers. Because the ion radius of  $\text{Cu}^{2+}$  is 1 pm smaller than  $\text{Zn}^{2+}$  and because the Jahn-Teller effect of  $\text{Cu}(\text{OH})_6$  octahedral units can further shorten the Cu-O bond length on the  $xy$  plane, the incorporation of  $\text{Cu}^{2+}$  is accompanied by a decrease in the cation-cation distance [27,32]. A schematic diagram of structural and composition changes to the LDHs before and after the *in situ* reduction is shown in Fig. S1 [33]. The  $\text{Cu}_2\text{O}$  phase formed after the Cu-Zn-Cr LDHs were reacted with ascorbic acid, and the amount of  $\text{Cu}_2\text{O}$  increased with increasing  $x$ , as did the crystallinity. In addition, the LDH phases remain after the reactions. However, a large amount of  $\text{Cu}^{2+}$  was separated out, and the intensity of the diffraction peaks decreased and became broad, reflecting the decrease in the crystallinity of the LDH phase. After reduction, the (110) and (113) peaks attributed to LDH phases were generally still coincided with the reflections of the ternary LDH matrixes. Because  $\text{Cu}^{2+}$  and the interlayer counter ion  $\text{CO}_3^{2-}$  have the same valence number, LDHs can maintain the charge balance as well as the crystal structure by dissociating a  $\text{Cu}^{2+}$  and a  $\text{CO}_3^{2-}$  simultaneously during the *in situ* reduction. Lattice defects of LDH backbones possibly generated in the process.

To confirm how the separating out of  $\text{Cu}^{2+}$  affected the surface area of the photocatalyst, the  $\text{N}_2$  adsorption-desorption isotherms of  $0.1\text{Cu}_2\text{O}@\text{Zn}_{1.8}\text{Cr}$  LDH and the corresponding  $\text{Cu}_{0.2}\text{Zn}_{1.8}\text{Cr}$  LDH were measured and plotted, as shown in Fig. S2. Both samples show hysteresis loops typical of mesoporous materials, but the adsorption volume ( $V_a$ ) at the same  $p/p_0$  of  $0.1\text{Cu}_2\text{O}@\text{Zn}_{1.8}\text{Cr}$  is obviously lower in the high-pressure area. Using the Kelvin equation, we found that the pore size decreased slightly after the *in situ* reduction. The specific surface area calculated by the Brunauer-Emmett-Teller (BET) method before and after the *in situ* reduction were 133 and  $123 \text{ m}^2 \text{ g}^{-1}$ , respectively. Although the specific surface area decreased with increasing separation of  $\text{Cu}^{2+}$ , the value is still within the normal range of LDHs [2].

As shown in the TEM images in Fig. 2, the samples have a morphology consisting of accumulated sheet-like structures. The shape of the brucite-like layers is maintained after the *in situ* reduction, but some independent particles are observed. The high resolution TEM images D2 and E2 show the distinct lattice fringes with a d-spacing of 0.29 nm, which is corresponding to the (110) lattice planes of cubic crystal structured  $\text{Cu}_2\text{O}$  [19,34]. The  $\text{Cu}_2\text{O}$  particle size at both  $x = 0.10$  and  $x = 0.20$  is lower than 30 nm, while agglomerated particles were observed at  $x = 0.40$ . With a lower Cu content, the growth of  $\text{Cu}_2\text{O}$  nuclei in the reduction reaction was restricted because of the surrounding brucite-like layers; consequently, the particles were quite small and highly dispersed in the LDH frameworks. In contrast, with an excessive Cu content, large numbers of  $\text{Cu}_2\text{O}$  nuclei separated out in the reduction reaction, gathering and growing into large crystals.

Fig. 3 shows the FT-IR spectra of several representative samples. All the spectra show broad and intense bands at about  $3400 \text{ cm}^{-1}$ , attributed to the stretching modes of the hydroxyl groups in the LDH host layers and interlayer water molecules. The band at  $1640 \text{ cm}^{-1}$  is assigned to the bending vibration of water. According to the symmetry group characteristics of the carbonate ion, the bands observed around  $1350$  and  $770 \text{ cm}^{-1}$  are, respectively, the  $\nu_3$  antisymmetric stretch and  $\nu_2$  out-of-plane bend [35]. In the low-frequency region, the fingerprints are attributed to the lattice vibrations from the LDH host layers. A weak band was also observed at  $630 \text{ cm}^{-1}$  for the  $0.4\text{Cu}_2\text{O}@\text{Zn}_{1.2}\text{Cr}$  LDH sample, and this is assigned to the Cu-O lattice vibration from the loaded  $\text{Cu}_2\text{O}$  particles [17,34]. The adsorbed organic contaminants derived from ascorbic acid in the *in situ* reduction process had a negative effect on the accuracy of  $\text{CO}_2$  photoreduction performance tests because they can easily decompose to C1 compounds under UV irradiation. However, here, the absence of stretching vibration bands corresponding to carbon-hydrogen ( $2960\text{--}2850 \text{ cm}^{-1}$ ) and carbonyl bonds ( $1820\text{--}1650 \text{ cm}^{-1}$ ) in the spectra suggests that the alkaline reaction condition effectively suppressed the ion exchange adsorption of ascorbic-acid-derived species on the LDHs [36].

Fig. 4 shows the UV-vis diffuse reflection spectra of some representative LDHs before and after the *in situ* reduction. The spectra

### Before *in situ* reduction ( $\text{Cu}_{2x}\text{Zn}_{2-2x}\text{Cr}$ LDH)

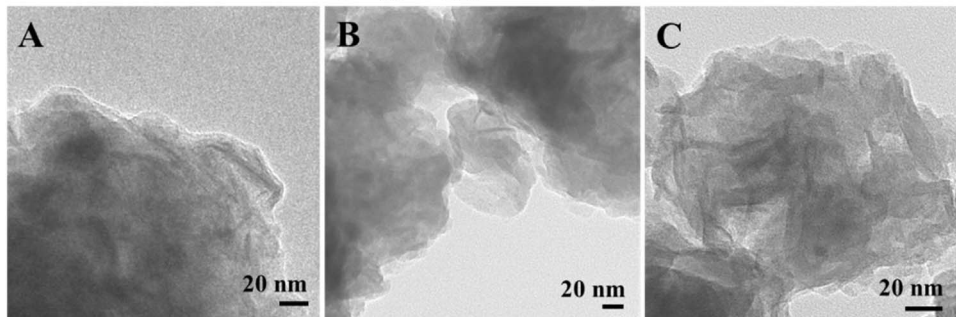


Fig. 2. TEM images of  $\text{Cu}_{2x}\text{Zn}_{2-2x}\text{Cr}$  LDH: A:  $x = 0.10$ ; B:  $x = 0.20$ ; C:  $x = 0.40$ , and the corresponding  $x\text{Cu}_2\text{O}@\text{Zn}_{2-2x}\text{Cr}$  LDH: D1, D2:  $x = 0.10$ ; E1, E2, E3:  $x = 0.20$ , where E3 is the image of two dimensional fast Fourier transform; and F:  $x = 0.40$ .

### After *in situ* reduction ( $x\text{Cu}_2\text{O}@\text{Zn}_{2-2x}\text{Cr}$ LDH)

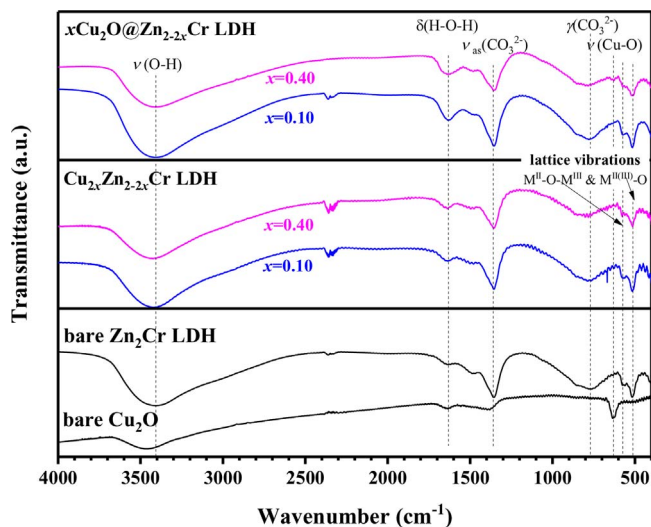
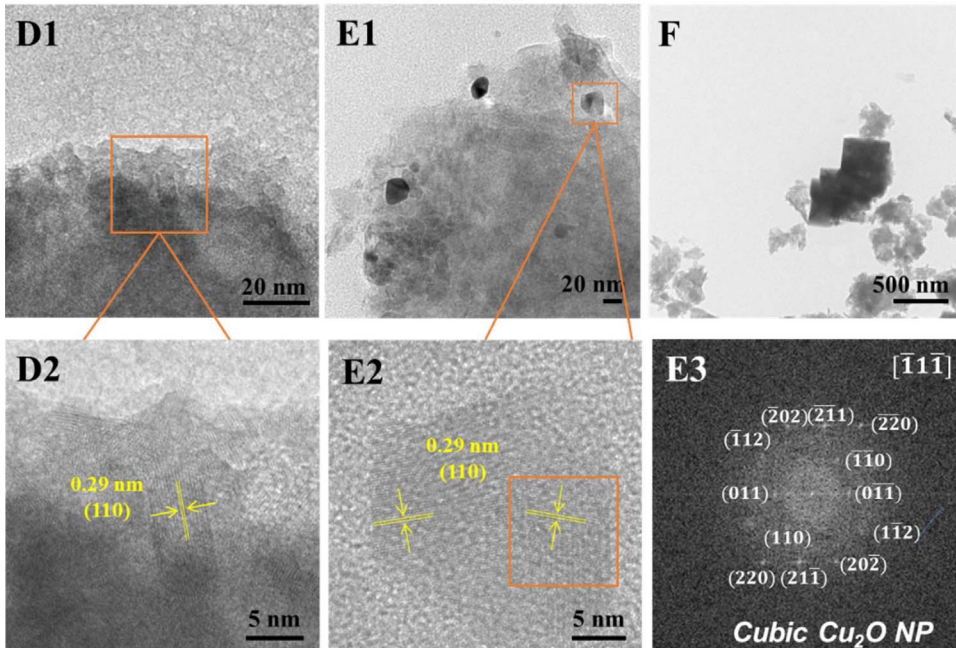


Fig. 3. FT-IR spectra of representative  $\text{Cu}_{2x}\text{Zn}_{2-2x}\text{Cr}$  LDHs ( $x = 0.10, 0.40$ ), the corresponding  $x\text{Cu}_2\text{O}@\text{Zn}_{2-2x}\text{Cr}$  LDH ( $x = 0.10, 0.40$ ), bare  $\text{Zn}_2\text{Cr}$  LDH, and bare  $\text{Cu}_2\text{O}$ .

were converted using the Kubelka–Munk function ( $F(R)$ ) from the reflectivity data. In the UV region, the pristine  $\text{Zn}_2\text{Cr}$  LDH displays the intrinsic absorption bands, which are attributed to the ligand–metal

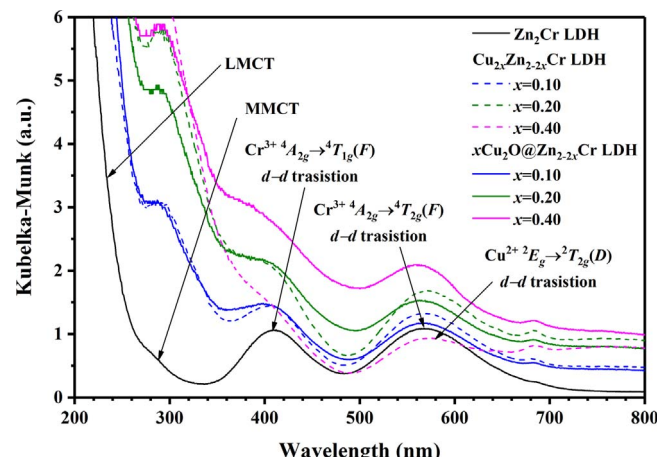
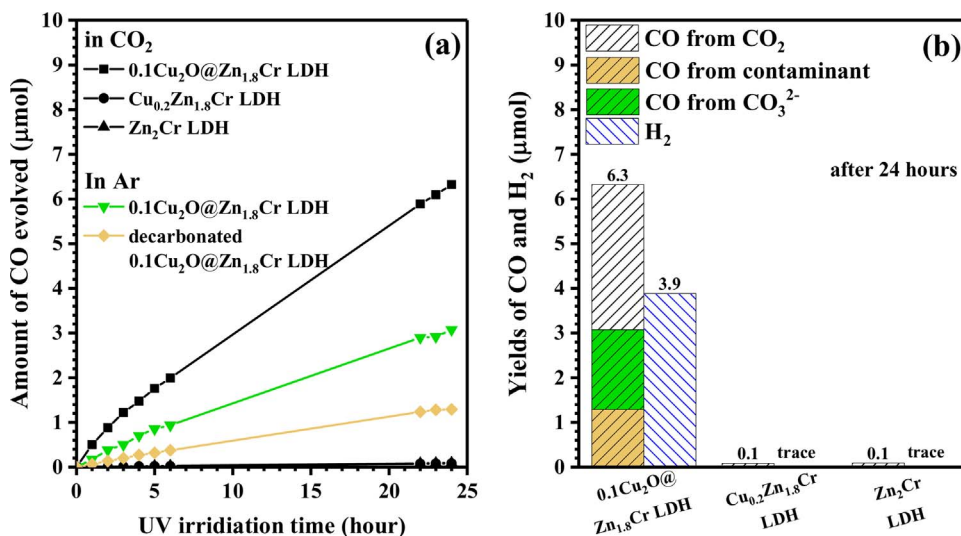


Fig. 4. UV-VIS DRS spectra of  $\text{Cu}_{2x}\text{Zn}_{2-2x}\text{Cr}$  LDH ( $x = 0.10, 0.20, 0.40$ ), and the corresponding  $x\text{Cu}_2\text{O}@\text{Zn}_{2-2x}\text{Cr}$  LDH ( $x = 0.10, 0.20, x = 0.40$ ).

charge transfer (LMCT) from the O  $2p$  orbital to the Zn  $4s$  and Cr  $3d(e_g)$  orbitals. The absorption band at 264–318 nm in the spectrum is attributed to metal–metal charge transfer (MMCT) from Cr  $3d(t_{2g})$  to Zn  $4s$  [22,37]. The absorption edge observed at 318 nm is corresponding to an approximate band gap ( $E_g$ ) of 3.9 eV. In the visible-light region, the



adsorption peaks at 410 and 570 nm correspond to the  $^4A_{2g} \rightarrow ^4T_{1g}(F)$  and  $^4A_{2g} \rightarrow ^4T_{2g}(F)$   $d-d$  transitions of the Cr<sup>3+</sup> ions, respectively [38]. The absorption spectra of the Cu-Zn-Cr ternary LDHs from 200 to 500 nm are complex but mainly consist of overlapped LMCT, MMCT, and Cr<sup>3+</sup>  $^4A_{2g} \rightarrow ^4T_{1g}(F)$   $d-d$  transitions. The overlap of the Cr<sup>3+</sup>  $^4A_{2g} \rightarrow ^4T_{2g}(F)$  and Cu<sup>2+</sup>  $^2E_g \rightarrow ^2T_{2g}(D)$   $d-d$  transitions redshifts the peaks around 570 nm gradually with increasing Cu<sup>2+</sup> content [39]. After the *in situ* reduction, the change of absorption characteristics in the UV region is attributed to the overlap of the intrinsic absorption of Cu<sub>2</sub>O. Around 570 nm, the influence of the Cu<sup>2+</sup>  $d-d$  transition disappeared, and the absorption peaks around 570 nm were blue-shifted to the same positions as those of the pristine Zn<sub>2</sub>Cr LDH. This indicates that Cu<sup>2+</sup> is not involved in the band structure of the LDHs after its reduction to Cu<sub>2</sub>O.

### 3.2. Photocatalytic performance

Fig. 5 shows a comparison of the photocatalytic activity among 0.1Cu<sub>2</sub>O@Zn<sub>1.8</sub>Cr LDH, ternary Cu<sub>0.2</sub>Zn<sub>1.8</sub>Cr LDH, and the pristine Zn<sub>2</sub>Cr LDH under a CO<sub>2</sub> atmosphere. The LDHs not loaded with Cu<sub>2</sub>O exhibited limited activity. The CO released after 24 h was approximately 0.1  $\mu\text{mol}$ , and a trace amount of H<sub>2</sub> in the pure water was observed. In contrast, 0.1Cu<sub>2</sub>O@Zn<sub>1.8</sub>Cr LDH exhibited a CO yield of up to 6.3  $\mu\text{mol}$ , and 3.9  $\mu\text{mol}$  of H<sub>2</sub> was generated simultaneously. To identify the activation effect of the Cu<sub>2</sub>O particles as narrow bandgap semiconductors, 0.1Cu<sub>2</sub>O@Zn<sub>1.8</sub>Cr LDH was also irradiated with visible light using a 200-W Xe lamp (LA-410UV, Hayashi Watch-works) with a 400-nm cutoff filter (SC 40, Fujifilm Corporation). The generation of H<sub>2</sub> and CO was not observed. Thus, the light harvesting material for the photocatalytic reaction is LDH, whereas Cu<sub>2</sub>O tends to act as the cocatalyst, accelerating the reaction. A series of control tests was carried out to verify whether CO is derived from CO<sub>2</sub> by repeating the UV irradiation of 0.1Cu<sub>2</sub>O@Zn<sub>1.8</sub>Cr LDH under an Ar atmosphere. Considering that the interlayer CO<sub>3</sub><sup>2-</sup> ions are also a possible carbon source because they can transform to CO<sub>2</sub> via hydrolysis, a portion of the 0.1Cu<sub>2</sub>O@Zn<sub>1.8</sub>Cr LDH was decarbonized via an ion-exchange process in a NaH<sub>2</sub>PO<sub>4</sub> aqueous solution prior to the irradiation tests in Ar. The amount of CO generated on the CO<sub>3</sub><sup>2-</sup>-type and decarbonized samples were 3.1 and 1.3  $\mu\text{mol}$ , respectively (Fig. 5(b)). This indicates that almost 80% of the CO production is assigned to the reduction of CO<sub>2</sub> but not the incomplete oxidation product of the surface-adsorbed organic contaminants. The isotope analysis result shows the obvious and ever-increasing mass spectra peaks of <sup>18</sup>O<sub>2</sub> ( $m/z = 36$ ) and <sup>13</sup>CO ( $m/z = 29$ ) after irradiating the 0.1Cu<sub>2</sub>O@Zn<sub>1.8</sub>Cr LDH impregnated with H<sub>2</sub><sup>18</sup>O under a <sup>13</sup>CO<sub>2</sub> atmosphere with UV light (Fig. 6). We confirmed that the

photogenerated electrons reduced CO<sub>2</sub> to CO and the holes oxidized water to oxygen simultaneously. Evidently, after the modification of Cu<sub>2</sub>O nanoparticles on the LDH surface, the photocatalytic performance was enhanced significantly. This result indicates that Cu<sub>2</sub>O can serve as an electron trap, reducing the recombination of photogenerated electrons and holes and increasing the photocatalytic efficiency. Meanwhile, Cu<sub>2</sub>O nanoparticles are probably quite sensitive to CO<sub>2</sub>, and they can function as reaction sites, promoting the conversion of CO<sub>2</sub> to CO (Fig. 7).

The effect of the Cu content on the photocatalytic activity is shown in Fig. 8. All the Cu<sub>2</sub>O-decorated samples showed activity for the reduction of CO<sub>2</sub> to CO, accompanied by water splitting, generating H<sub>2</sub> as a side reaction. The production of CO increased linearly with the irradiation time. The 0.1Cu<sub>2</sub>O@Zn<sub>1.8</sub>Cr LDH sample exhibited the highest yields of CO and H<sub>2</sub>, but the selectivity toward CO generation was only 62.3%. The 0.2Cu<sub>2</sub>O@Zn<sub>1.6</sub>Cr LDH displayed the highest selectivity of 82.3%, but the yield of CO (4.1  $\mu\text{mol}$ ) was inferior to that of the 0.1Cu<sub>2</sub>O@Zn<sub>1.8</sub>Cr LDH. The 0.4Cu<sub>2</sub>O@Zn<sub>1.2</sub>Cr LDH, which has the highest Cu<sub>2</sub>O content, showed the lowest yields of both CO (2.3  $\mu\text{mol}$ ) and H<sub>2</sub> (0.5  $\mu\text{mol}$ ). This suggests that excess Cu<sub>2</sub>O loading may reduce the synergism between LDHs and Cu<sub>2</sub>O because of the formation of large particles and the poor dispersion of Cu<sub>2</sub>O in the LDH frameworks. In addition, a large quantity of Cu<sub>2</sub>O particles can mask the LDH surface, reducing the photoexcitation of the LDHs and suppressing the photocatalytic efficiency [40].

The effect of additives on the photocatalytic activity of the 0.1Cu<sub>2</sub>O@Zn<sub>1.8</sub>Cr LDH was also studied. As shown in Fig. 9, the addition of Na<sub>2</sub>SO<sub>3</sub> severely suppressed the formation of CO but increased the generation of H<sub>2</sub>, which increased to 41.2  $\mu\text{mol}$  after 24-h irradiation, 11.8 times higher than the case without any additive. The addition of Na<sub>2</sub>CO<sub>3</sub> also suppressed the generation of CO. SO<sub>3</sub><sup>2-</sup> is an ideal hole scavenger and promotes the water splitting reaction. The reason for the decreased CO generation is probably that CO<sub>3</sub><sup>2-</sup> and SO<sub>3</sub><sup>2-</sup> occupied the CO<sub>2</sub> adsorption sites and then inhibited the adsorption and reduction reactions on the surface of the photocatalyst. The addition of NaCl weakened both the CO<sub>2</sub> reduction and water splitting reactions slightly but improved the selectivity toward CO generation. Notably, using a CO<sub>2</sub> UFB solution instead of water can improve both the CO production and the selectivity, indicating that the increase in CO<sub>2</sub> solubility significantly increases the photocatalytic activity for CO<sub>2</sub> reduction.

The chemical stability of Cu<sub>2</sub>O-loaded LDH was investigated. During the photocatalytic reaction, it was observed the photocatalyst turned black gradually. The redox potential of CuO/Cu<sub>2</sub>O is +0.193 V (vs. SHE, pH = 7), within the region between the valence band (VB) top and conduction band (CB) bottom of Cu<sub>2</sub>O [41]. This is possibly

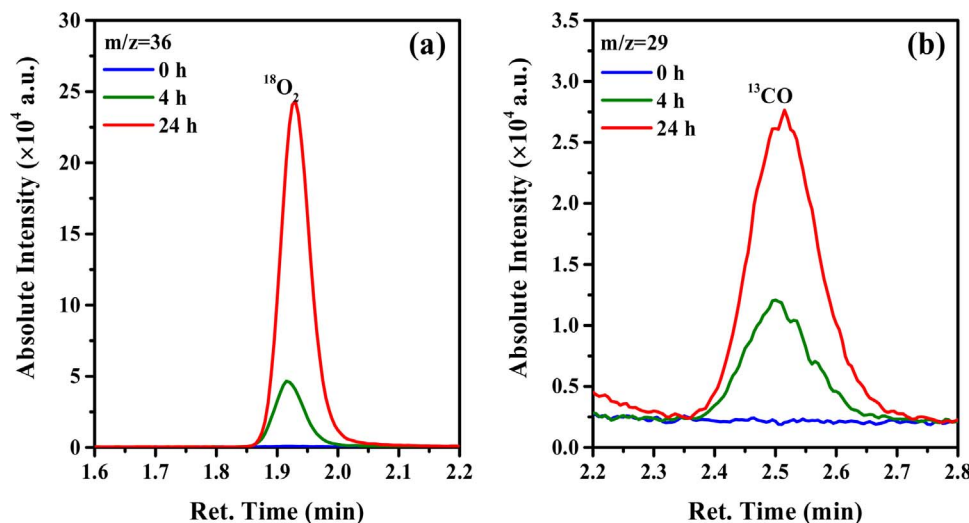


Fig. 6. Mass chromatography spectra of (a)  $^{18}\text{O}_2$  ( $m/z = 36$ ) and (b)  $^{13}\text{CO}$  ( $m/z = 29$ ) generated on  $0.1\text{Cu}_2\text{O}@\text{Zn}_{1.8}\text{Cr}$  LDH impregnated with  $\text{H}_2^{18}\text{O}$  under  $^{13}\text{CO}_2$  atmosphere.

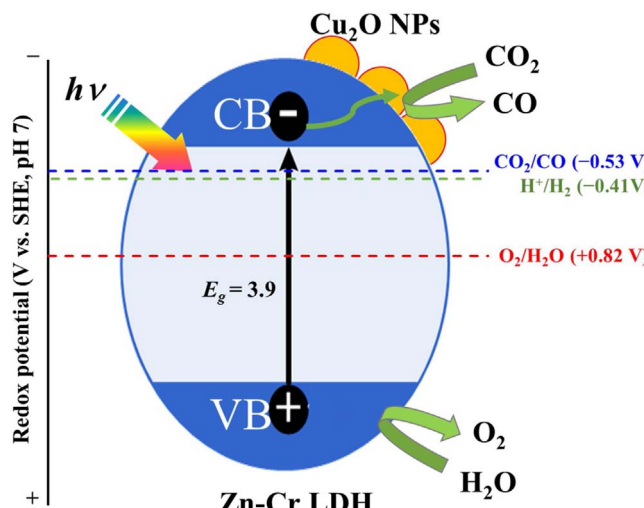


Fig. 7. Estimated electron transfer mode from Zn-Cr LDH to  $\text{Cu}_2\text{O}$ .

because part of the  $\text{Cu}^{\text{I}}$  was self-oxidized to  $\text{Cu}^{\text{II}}$  under UV irradiation, forming mixed-valence  $\text{Cu}_x\text{O}$  species, which might be the active species, resulting in enhanced photocatalytic activity [42]. Gunjakar et al. [43] suggested a charge transfer mode from Zn-Cr LDH to other semiconductors such as layered titanate. Zn-Cr LDHs can be regarded as

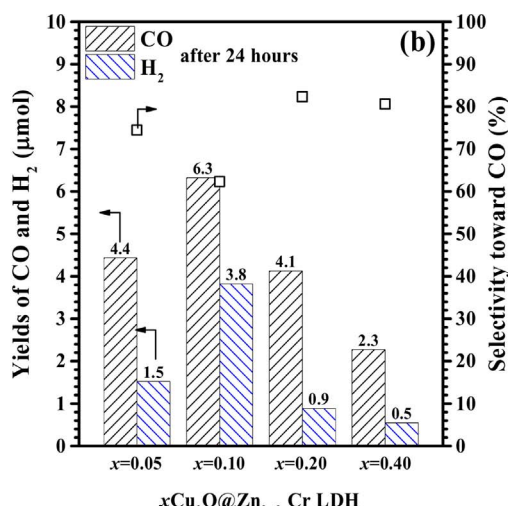
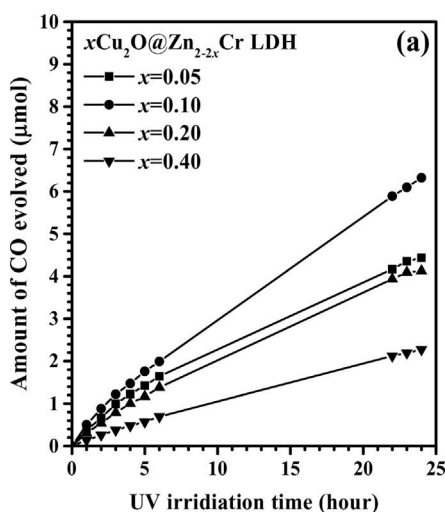


Fig. 9. Effect of additives on the CO and  $\text{H}_2$  output in the  $\text{CO}_2$  photoreduction reaction using  $0.1\text{Cu}_2\text{O}@\text{Zn}_{1.8}\text{Cr}$  LDH as the photocatalyst.

wide band semiconductor-like species, whose CB bottom and interstate bands are sufficiently negative to afford electron transfer to the CB of layered titanate. In contrast,  $\text{Cu}_2\text{O}$  has a quite negative CB, which is unlikely able to accept the photogenerated electrons from the Zn-Cr LDHs. However, the self-oxidation of  $\text{Cu}^{\text{I}}$  under UV irradiation resulted

Fig. 9. Effect of additives on the CO and  $\text{H}_2$  output in the  $\text{CO}_2$  photoreduction reaction using  $0.1\text{Cu}_2\text{O}@\text{Zn}_{1.8}\text{Cr}$  LDH as the photocatalyst.

in the Fermi level shifting in the positive direction and the formation of unoccupied Cu 3d orbitals below the CB of Cu<sub>2</sub>O. These changes probably allow the electron transfer from the CB of Zn-Cr LDHs to the unoccupied Cu 3d orbitals of the surface-loaded Cu<sub>2</sub>O nanoparticles, which are also highly active reaction sites for CO evolution from CO<sub>2</sub> in aqueous solution. The XRD patterns of the representative planes in 0.1Cu<sub>2</sub>O@Zn<sub>1.8</sub>Cr LDH before and after the CO<sub>2</sub> photoreduction reaction are also recorded for the further analysis of its chemical stability. Fig. S3(a) shows LDH phase are well preserved, and its crystallinity has not been changed. However, as shown in Fig. S3(b), the diffraction peaks of both Cu<sub>2</sub>O and Cu existed after the reaction, indicating part of Cu<sub>2</sub>O was self-reduced by photoelectrons. It does not imply that the photocatalyst will be out of activity, because Cu can also serve as a reaction site for CO<sub>2</sub> photoreduction [44–46]. Fig. S4 shows the average formation rate of CO on Cu<sub>2</sub>O-loaded Zn-Cr LDHs at different time in CO<sub>2</sub> photoreduction reaction in pure water. In the initial stage, the formation rate of CO decreased along with the gradual reduction of Cu<sup>+</sup> to Cu<sup>0</sup>, attesting the fact Cu<sub>2</sub>O is more effective than Cu, which is consistent with the previous report [47]. The change between Cu<sup>+</sup> and Cu<sup>0</sup> was reversible and probably close to equilibrium after 4 h when the formation rate of CO turned into stable.

#### 4. Conclusions

The incorporation of copper oxides with LDHs is considered an effective approach to improve the activity of photocatalysts for the reduction of CO<sub>2</sub>. In this work, a series of Cu<sub>2</sub>O-decorated Zn-Cr LDHs (xCu<sub>2</sub>O@Zn<sub>2-x</sub>Cr LDH) were prepared via an *in situ* reduction process from the corresponding Cu-Zn-Cr ternary LDH with the same Cu content (Cu<sub>2x</sub>Zn<sub>2-2x</sub>Cr LDH). The formation of Cu<sub>2</sub>O nanoparticles and preservation of the LDH structure was confirmed. The 0.1Cu<sub>2</sub>O@Zn-Cr LDH exhibited the best activity among the loaded LDHs, and the activity was superior to the corresponding Cu-Zn-Cr ternary LDH and pristine Zn<sub>2</sub>Cr LDHs. The loaded Cu<sub>2</sub>O nanoparticles probably function as effective electron traps, promoting charge separation and providing active sites for CO<sub>2</sub> reduction. This study provides a simple and efficient approach for the fabrication of high-performance LDH-based artificial photosynthesis systems.

#### Acknowledgements

The authors are grateful to Prof. Y. Kitamoto (Tokyo Institute of Technology, Japan) for the provision of TEM instrument. This work was supported in part by “Grant-in-Aid for Young Scientists (A; 25708037)” from Japan Society for the Promotion of Science (JSPS).

#### Appendix A. Supplementary data

Supplementary data associated with this article can be found, in the online version, at <http://dx.doi.org/10.1016/j.apcatb.2017.11.011>.

#### References

- [1] X. Duan, D.G. Evans, Layered Double Hydroxides, Springer Science & Business Media, Berlin, 2006.
- [2] F. Li, X. Duan, Applications of layered double hydroxides, in: X. Duan, D.G. Evans (Eds.), Layer. Double Hydroxides, Springer Berlin Heidelberg, Berlin, 2006, pp. 193–223.
- [3] A.I. Khan, D. O’Hare, Intercalation chemistry of layered double hydroxides: recent developments and applications, *J. Mater. Chem.* 12 (2002) 3191–3198.
- [4] N. Ahmed, Y. Shibata, T. Taniguchi, Y. Izumi, Photocatalytic conversion of carbon dioxide into methanol using zinc-copper-M(III) (M = aluminum, gallium) layered double hydroxides, *J. Catal.* 279 (2011) 123–135.
- [5] K. Teramura, S. Iguchi, Y. Mizuno, T. Shishido, T. Tanaka, Photocatalytic conversion of CO<sub>2</sub> in water over layered double hydroxides, *Angew. Chem. Int. Ed.* 51 (2012) 8008–8011.
- [6] S. Iguchi, K. Teramura, S. Hosokawa, T. Tanaka, Effect of the chloride ion as a hole scavenger on the photocatalytic conversion of CO<sub>2</sub> in an aqueous solution over Ni-Al layered double hydroxides, *Phys. Chem. Chem. Phys.* 17 (2015) 17995–18003.
- [7] S. Iguchi, K. Teramura, S. Hosokawa, T. Tanaka, Photocatalytic conversion of CO<sub>2</sub> in an aqueous solution using various kinds of layered double hydroxides, *Catal. Today* 251 (2015) 140–144.
- [8] S. Iguchi, S. Kikkawa, K. Teramura, S. Hosokawa, T. Tanaka, Investigation of the electrochemical and photoelectrochemical properties of Ni-Al LDH photocatalysts, *Phys. Chem. Chem. Phys.* 18 (2016) 13811–13819.
- [9] K. Iizuka, T. Wato, Y. Miseki, K. Saito, A. Kudo, Photocatalytic reduction of carbon dioxide over Ag cocatalyst-loaded Al<sub>x</sub>Ti<sub>4</sub>O<sub>15</sub> (A = Ca Sr, and Ba) using water as a reducing reagent, *J. Am. Chem. Soc.* 133 (2011) 20863–20868.
- [10] S. Wang, Y. Hou, X. Wang, Development of a Stable MnCo<sub>2</sub>O<sub>4</sub> cocatalyst for photocatalytic CO<sub>2</sub> reduction with visible light, *ACS Appl. Mater. Interfaces* 7 (2015) 4327–4335.
- [11] K. Katsumata, K. Sakai, K. Ikeda, G. Carja, N. Matsushita, K. Okada, Preparation and photocatalytic reduction of CO<sub>2</sub> on noble metal (Pt, Pd, Au) loaded Zn-Cr layered double hydroxides, *Mater. Lett.* 107 (2013) 138–140.
- [12] I. Tseng, J.C.S. Wu, H. Chou, Effects of sol-gel procedures on the photocatalysis of Cu/TiO<sub>2</sub> in CO<sub>2</sub> photoreduction, *J. Catal.* 221 (2004) 432–440.
- [13] Q. Zhai, S. Xie, W. Fan, Q. Zhang, Y. Wang, W. Deng, Y. Wang, Photocatalytic conversion of carbon dioxide with water into methane: platinum and copper(i) oxide co-catalysts with a core-shell structure, *Angew. Chem.* 125 (2013) 5882–5891.
- [14] G. Yin, M. Nishikawa, Y. Nosaka, N. Srinivasan, D. Atarashi, E. Sakai, M. Miyauchi, Photocatalytic carbon dioxide reduction by copper oxide nanocluster-grafted niobate nanosheets, *ACS Nano.* 9 (2015) 2111–2119.
- [15] S. Shoji, G. Yin, M. Nishikawa, D. Atarashi, E. Sakai, M. Miyauchi, Photocatalytic reduction of CO<sub>2</sub> by Cu<sub>2</sub>O nanocluster loaded SrTiO<sub>3</sub> nanorod thin film, *Chem. Phys. Lett.* 658 (2016) 309–314.
- [16] Y. Pu, W. Lin, Y. Hsu, Modulation of charge carrier dynamics of Na<sub>x</sub>H<sub>2-x</sub>Ti<sub>3</sub>O<sub>7</sub>-Au-Cu<sub>2</sub>O Z-scheme nanoheterostructures through size effect, *Appl. Catal. B Environ.* 163 (2015) 343–351.
- [17] C. Lu, L. Qi, J. Yang, X. Wang, D. Zhang, J. Xie, J. Ma, One-Pot Synthesis of octahedral Cu<sub>2</sub>O nanocages via a catalytic solution route, *Adv. Mater.* 17 (2005) 2562–2567.
- [18] L. Gou, C.J. Murphy, Solution-phase synthesis of Cu<sub>2</sub>O nanocubes, *Nano Lett.* 3 (2003) 231–234.
- [19] W. Huang, L. Lyu, Y. Yang, M. Huang, Synthesis of Cu<sub>2</sub>O nanocrystals from cubic to rhombic dodecahedral structures and their comparative photocatalytic activity, *J. Am. Chem. Soc.* 134 (2012) 1261–1267.
- [20] W. Wang, G. Wang, X. Wang, Y. Zhan, Y. Liu, C. Zheng, Synthesis and characterization of Cu<sub>2</sub>O nanowires by a novel reduction route, *Adv. Mater.* 14 (2002) 67–69.
- [21] J. Ma, J. Ding, L. Li, J. Zou, Y. Kong, S. Komarneni, In situ reduction for synthesis of nano-sized Cu<sub>2</sub>O particles on MgCuAl-LDH layers for degradation of orange II under visible light, *Ceram. Int.* 41 (2015) 3191–3196.
- [22] N. Baliaj Singh, L. Mohapatra, K. Parida, Design and development of a visible light harvesting Ni-Zn-Cr-CO<sub>3</sub><sup>2-</sup> LDH system for hydrogen evolution, *J. Mater. Chem. A* 1 (2013) 4236–4243.
- [23] N. Baliaj Singh, K.M. Parida, G.C. Pradhan, Effects of Co, Ni Cu, and Zn on Photophysical and photocatalytic properties of carbonate intercalated mii/cr ldhs for enhanced photodegradation of methyl orange, *Ind. Eng. Chem. Res.* 53 (2014) 3834–3841.
- [24] G. Zhang, B. Lin, W. Yang, S. Jiang, Q. Yao, Y. Chen, B. Gao, Highly efficient photocatalytic hydrogen generation by incorporating CdS into ZnCr-layered double hydroxide interlayer, *RSC Adv.* 5 (2014) 5823–5829.
- [25] N. Hirata, K. Tadanaga, M. Tatsumisago, Photocatalytic O<sub>2</sub> evolution from water over Zn-Cr layered double hydroxides intercalated with inorganic anions, *Mater. Res. Bull.* 62 (2015) 1–4.
- [26] S. Ali Khan, S. Bahadar Khan, A.M. Asiri, Toward the design of Zn-Al and Zn-Cr LDH wrapped in activated carbon for the solar assisted de-coloration of organic dyes, *RSC Adv.* 6 (2016) 83196–83208.
- [27] R.D. Shannon, Revised effective ionic radii and systematic studies of interatomic distances in halides and chalcogenides, *Acta Crystallogr. Sect. A* 32 (1976) 751–767.
- [28] Y. Lu, W. Lin, C. Yang, Y. Chiu, Y. Pu, M. Lee, Y. Tseng, Y. Hsu, A facile green antisolvent approach to Cu<sup>2+</sup>-doped ZnO nanocrystals with visible-light-responsive photoactivities, *Nanoscale* 6 (2014) 8796–8803.
- [29] S. Miyata, The syntheses of hydrotalcite-like compounds and their structures and physico-chemical properties i: the systems Mg<sup>2+</sup>-Al<sup>3+</sup>-NO<sub>3</sub><sup>-</sup>, Mg<sup>2+</sup>-Al<sup>3+</sup>-Cl<sup>-</sup>, Mg<sup>2+</sup>-Al<sup>3+</sup>-ClO<sub>4</sub><sup>-</sup>, Ni<sup>2+</sup>-Al<sup>3+</sup>-Cl<sup>-</sup> and Zn<sup>2+</sup>-Al<sup>3+</sup>-Cl<sup>-</sup>, *Clays Clay Miner.* 23 (1975) 369–375.
- [30] C. Taviot-Guého, F. Leroux, C. Payen, J. Besse, Cationic ordering and second-stacking structures in copper-chromium and zinc-chromium layered double hydroxides, *Appl. Clay Sci.* 28 (2005) 111–120.
- [31] O. Clause, M. Gazzano, F. Trifirò, A. Vaccari, L. Zatorski, Preparation and thermal reactivity of nickel/chromium and nickel/aluminium hydrotalcite-type precursors, *Appl. Catal.* 73 (1991) 217–236.
- [32] L. Wang, W. Shi, P. Yao, Z. Ni, Y. Li, J. Liu, Microstructure and Jahn-Teller effect of Cu-Zn-Mg-Al layered double hydroxides, *Acta Phys.-Chim. Sin.* 28 (2012) 58–64.
- [33] K. Momma, F. Izumi, VESTA 3 for three-dimensional visualization of crystal, volumetric and morphology data, *J. Appl. Crystallogr.* 44 (2011) 1272–1276.
- [34] Y. Pu, H. Chou, W. Kuo, K. Wei, Y. Hsu, Interfacial charge carrier dynamics of cuprous oxide-reduced graphene oxide (Cu<sub>2</sub>O-rGO) nanoheterostructures and their related visible-light-driven photocatalysis, *Appl. Catal. B Environ.* 204 (2017) 21–32.
- [35] S.J. Palmer, T. Nguyen, R.L. Frost, Synthesis and Raman spectroscopic characterisation of hydrotalcite with CO<sub>3</sub><sup>2-</sup> and VO<sub>3</sub><sup>-</sup> anions in the interlayer, *J. Raman Spectrosc.*

Spectrosc. 38 (2007) 1602–1608.

[36] National Astronomical Observatory of Japan, Chronological Scientific Tables 2015, Maruzen Publishing Co., Ltd, Tokyo, 2014.

[37] R. Nakamura, A. Okamoto, H. Osawa, H. Irie, K. Hashimoto, Design of all-inorganic molecular-based photocatalysts sensitive to visible light: Ti(IV)-O-Ce(III) bimetallic assemblies on mesoporous silica, *J. Am. Chem. Soc.* 129 (2007) 9596–9597.

[38] A. Ceulemans, B. Coninckx, C. Görller-Walrand, H. Jacobs, J. Bock, The ligand field spectrum of  $K_3[Cr(OH)_6]$ , *Chem. Phys. Lett.* 150 (1988) 127–128.

[39] N.L.D. Filho, Adsorption of Cu(II) and Co(II) complexes on a silica gel surface chemically modified with 2-mercaptoimidazole, *Microchim. Acta* 130 (1999) 233–240.

[40] H. Li, C. Li, L. Han, C. Li, S. Zhang, Photocatalytic reduction of  $CO_2$  with  $H_2O$  on  $CuO/TiO_2$  catalysts, *Energy Sources Part Recovery Util. Environ.* 38 (2016) 420–426.

[41] Y. Yang, J. Han, X. Ning, J. Su, J. Shi, W. Cao, W. Xu, Photoelectrochemical stability improvement of cuprous oxide ( $Cu_2O$ ) thin films in aqueous solution, *Int. J. Energy Res.* 40 (2016) 112–123.

[42] L. Liu, C. Zhao, J.T. Miller, Y. Li, Mechanistic Study of  $CO_2$  Photoreduction with  $H_2O$  on  $Cu/TiO_2$  nanocomposites by in situ X-ray absorption and infrared spectroscopies, *J. Phys. Chem. C* 121 (2017) 490–499.

[43] J.L. Gunjakar, T.W. Kim, H.N. Kim, I.Y. Kim, S.-J. Hwang, Mesoporous layer-by-layer ordered nanohybrids of layered double hydroxide and layered metal oxide: highly active visible light photocatalysts with improved chemical stability, *J. Am. Chem. Soc.* 133 (2011) 14998–15007.

[44] Y. Li, W. Wang, Z. Zhan, M. Woo, C. Wu, P. Biswas, Photocatalytic reduction of  $CO_2$  with  $H_2O$  on mesoporous silica supported  $Cu/TiO_2$  catalysts, *Appl. Catal. B Environ.* 100 (2010) 386–392.

[45] B. Chen, V. Nguyen, J.C.S. Wu, R. Martin, K. Kočí, Production of renewable fuels by the photohydrogenation of  $CO_2$ : effect of the Cu species loaded onto  $TiO_2$  photocatalysts, *Phys. Chem. Chem. Phys.* 18 (2016) 4942–4951.

[46] G. Yin, H. Abe, R. Kodiyath, S. Ueda, N. Srinivasan, A. Yamaguchi, M. Miyauchi, Selective electro- or photo-reduction of carbon dioxide to formic acid using a Cu-Zn alloy catalyst, *J. Mater. Chem. A* 5 (2017) 12113–12119.

[47] Z. Xiong, Z. Lei, C. Kuang, X. Chen, B. Gong, Y. Zhao, J. Zhang, C. Zheng, J.C.S. Wu, Selective photocatalytic reduction of  $CO_2$  into  $CH_4$  over  $Pt-Cu_2O/TiO_2$  nanocrystals: the interaction between Pt and  $Cu_2O$  cocatalysts, *Appl. Catal. B Environ.* 202 (2017) 695–703.